Video Article

A Mouse Fetal Skin Model of Scarless Wound Repair

Graham G. Walmsley*[1,2], Michael S. Hu*[1,2,3], Wan Xing Hong[1,4], Zeshaan N. Maan[1], H. Peter Lorenz[1], Michael T. Longaker[1,2]

[1]Hagey Laboratory for Pediatric Regenerative Medicine, Department of Surgery, Division of Plastic and Reconstructive Surgery, Stanford University School of Medicine

[2]Institute for Stem Cell Biology and Regenerative Medicine, Stanford University School of Medicine

[3]Department of Surgery, John A. Burns School of Medicine, University of Hawai'i

[4]University of Central Florida College of Medicine

*These authors contributed equally

Correspondence to: Michael T. Longaker at longaker@stanford.edu

URL: https://www.jove.com/video/52297
DOI: doi:10.3791/52297

Keywords: Medicine, Issue 95, fetal surgery, scarless, scar, wound healing, regeneration, skin, fibrosis

Date Published: 1/16/2015

Citation: Walmsley, G.G., Hu, M.S., Hong, W.X., Maan, Z.N., Lorenz, H.P., Longaker, M.T. A Mouse Fetal Skin Model of Scarless Wound Repair. *J. Vis. Exp.* (95), e52297, doi:10.3791/52297 (2015).

Abstract

Early *in utero*, but not in postnatal life, cutaneous wounds undergo regeneration and heal without formation of a scar. Scarless fetal wound healing occurs across species but is age dependent. The transition from a scarless to scarring phenotype occurs in the third trimester of pregnancy in humans and around embryonic day 18 (E18) in mice. However, this varies with the size of the wound with larger defects generating a scar at an earlier gestational age. The emergence of lineage tracing and other genetic tools in the mouse has opened promising new avenues for investigation of fetal scarless wound healing. However, given the inherently high rates of morbidity and premature uterine contraction associated with fetal surgery, investigations of fetal scarless wound healing *in vivo* require a precise and reproducible surgical model. Here we detail a reliable model of fetal scarless wound healing in the dorsum of E16.5 (scarless) and E18.5 (scarring) mouse embryos.

Video Link

The video component of this article can be found at https://www.jove.com/video/52297/

Introduction

Fetal skin wounds heal rapidly and scarlessly until late in gestation[1]. Fetal scarless wound repair is characterized by regeneration of normal tissue architecture and function. The transition from a scarless to scarring phenotype occurs in the third trimester of pregnancy in humans and around embryonic day 18 (E18) in mice[2,3]. In comparison to adult, fetal wound repair is characterized by rapid epithelialization, connective tissue deposition, and fibroblast migration.

Many studies have offered possible explanations for the phenomenon of scarless wound healing during early fetal development. Inflammation is a fundamental component of adult wound repair; however, fetal wounds are characterized by a lack of acute inflammation[4]. Whether this is a consequence of the functional immaturity of the immune system during fetal stages remains unclear. A recent study suggested that differences in the abundance, maturity, and function of mast cells in E15 vs. E18 fetal skin may be responsible for the transition from a scarless phenotype, at least in the mouse[3]. Other studies posit that differences in the properties and abundance of fetal and adult wound macrophages are responsible for the reformation of normal extracellular matrix (ECM) during fetal wound repair[5].

Differences in environmental factors during fetal and adult development may also affect wound repair. Longaker and colleagues showed that wound fluid from the fetus possesses high levels of hyaluronic acid-stimulating activity compared to none in adult wound fluid[6]. Consequently, higher levels of hyaluronic acid, a glycosaminoglycan that promotes a microenvironment conducive to cell motility and proliferation, in the fetal wound environment may be responsible for the scarless phenotype seen during early fetal development. Other lines of evidence point to the fact that the fetal wound environment is relatively hypoxemic and submerged in sterile amniotic fluid rich in growth factors[7]. However, no definitive answer has been provided for a critical event or factor during embryogenesis that triggers the transition from scarless regeneration to fibrotic repair.

Understanding the mechanisms responsible for scarless healing in the fetus necessitates a precise and reproducible model. Here we detail a reproducible model of fetal scarless wound healing in the dorsum of E16.5 (scarless) and E18.5 (scarring) mouse embryos. Additionally, minor variations of this model can be utilized to perform a number of further studies, such as gene expression analysis of fetal wounds and skin[8,9]. Given that precisely timed pregnancies are critical for successful recapitulation of this fetal scarless wound healing model, we also detail our protocol for superovulation timed pregnancies.

Protocol

NOTE: All procedures described in this paper are performed according to guidelines established by the Stanford Administrative Panel on Laboratory Animal Care (APLAC).

1. Timed Pregnancies – Superovulation Technique (Figure 1)

NOTE: Precisely timing the gestational age of mouse embryos for fetal surgery at E16.5 and E18.5 is of critical importance. In this section we detail our protocol for timing mouse pregnancies using pregnant mares serum (PMS) and human chorionic gonadotropin (HCG) injections to induce superovulation.

1. Inject female mice (<5 per cage) intraperitoneally (IP) with 3.0-5.0 international units (IU) of PMS in a volume of 100 µl PBS between 1:00 and 3:00 PM for day 1.
2. Between 12:00 and 2:00 PM of day 3 (forty-five to 47 hr after PMS injection), inject female mice IP with 3.0-5.0 IU of HCG in a volume of 100 µl PBS.
   NOTE: The HCG injection induces ovulation approximately 12 hr post-injection.
3. Immediately following HCG injections, mate females with males aged 8-16 weeks.
   NOTE: We typically place two females into a cage of individual males.
4. Separate females from males on the morning of day 4 (6:00 – 10:00 AM) and record as fetal age E0.5.
   NOTE: Vaginal plugs can be checked at this time; however, the observation of a vaginal plug does not guarantee pregnancy and females can become pregnant when no plug is observed. Given that pregnancy is typically observable by visual inspection and/or palpation at gestational ages E16.5 and E18.5, checking for vaginal plugs on the morning of day 4 is not strictly necessary. In our experience, and depending on the strain, approximately 30-50% of super-ovulated females become pregnant using the technique described here.

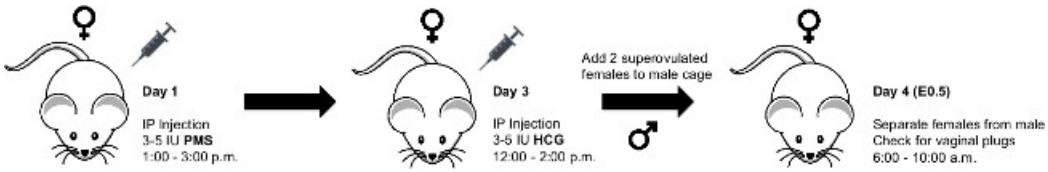

Figure 1. Schematic for Superovulation Technique. Schematic showing procedure for superovulation timed pregnancies in mice. Please click here to view a larger version of this figure.

2. Murine Fetal Surgery (Dorsal Wounding) on E16.5 and E18.5 Embryos (Figure 2)

1. Before the procedure, clean all surfaces of the operating room and equipment with 70% isopropyl alcohol. In addition, sterilize all surgical supplies and instruments that will be used in the procedure by autoclaving them. Some institutions may allow subsequent use of hot bead sterilization. Per operation, use sterile packs that include gauze and surgical instruments.
2. Induce anesthesia in pregnant mothers (fetal age E16.5 or E18.5) under 2.5% isoflurane/oxygen mixture at 2 L per min followed by maintenance anesthesia at 1 L per min.
3. To confirm proper anesthetization, ensure the deep pedal reflexes of the mouse are suppressed and place the mouse in the prone position.
4. Apply a vet ophthalmic ointment such as Puralube to prevent eye irritation or dryness during the procedure.
5. Prepare abdomen by administering a light application of depilatory cream for no longer than 30 sec (**Figure 2A**).
6. Prepare abdomen for aseptic surgery with povidone-iodine and alcohol (**Figure 2B and 2C**).
7. Perform midline laparotomy under microscope using microsurgical scissors (**Figure 2D and 2E**).
8. Gently expose uterus and fetus selected for surgery (**Figure 2F**).
9. Irrigate surgical field with warm (38 °C) phosphate-buffered saline (PBS) using a blunt-tip needle
   NOTE: One can be made by carefully bending the tip of a large-bore needle. (**Figure 2G and 2H**).
10. Position the fetus in a manner that allows full access to dorsum.
11. Pass a purse string stitch using 7-0 nylon suture through the uterus overlying the site of intended dorsal wounding (**Figure 2I**). Position purse string over a region of dorsum to the left or right of spinal cord, and in a region of uterine wall devoid of large blood vessels.
12. Make a 3 mm incision through uterine wall and amniotic sac in the center of the purse string (**Figure 2J**).
13. Irrigate incision site with warm (38 °C) PBS.
14. Using microsurgical scissors, cut a single full-thickness excisional wound, approximately 1 mm in length, in the dorsum of the fetus.
15. Gently blot incision site dry with cotton-tip applicator.
16. Inject 3 µl volume India ink subcutaneously into the wound site to mark location of wound (**Figure 2K**).
17. Irrigate with warm (38 °C) PBS to ensure ink has been retained within wound site.
18. Have surgical assistant inject warm (38 °C) PBS through blunt-tip 10 G syringe into the amniotic sac as the purse string is closed (**Figure 2L**). Retract syringe as purse string closure nears completion (**Figure 2M**).
19. Gently return uterus into the abdominal cavity (**Figure 2N**).
20. Evert skin and peritoneum.
21. Have surgical assistant irrigate abdominal cavity with warm (38 °C) PBS.
22. Close abdomen quickly by stapling skin and peritoneum closed (**Figure 2O**). The standard closure is performed in two layers; peritoneum and abdominal muscle in one layer, subcutaneous tissue and skin in the second layer. For immediate sacrifice and harvesting of the fetus, our demonstration shows closure in one layer.

23. Place the animal under observation in a warm incubator set at 37 °C for 30 min or until the animal regains sufficient consciousness to maintain sternal recumbency.
24. Do not return the animal to the company of other animals until it has fully recovered from the procedure.
25. Upon awaking from anesthesia and during the subsequent 48 hr, administer subcutaneous injection of buprenorphine (0.05 mg/kg) every 12 hr for analgesia as needed based on pain assessment. Administer carprofen (5 mg/kg) via subcutaneous injection for additional post-operative pain relief as needed.
26. Return animals to the cage and provide them with food and water ad libitum.
27. Monitor closely for manifestations of pain.
28. 48 hr post-surgery, sacrifice pregnant mother with an overdose of isoflurane and harvest wounded fetus. In order to do this, adjust isoflurane concentration to 5% or higher and maintain exposure for 1 min after cessation of breathing. Confirm euthanasia with cervical dislocation. Harvest an unwounded embryo for age-matched control. Late embryos should have a separate method of euthanasia consistent with IACUC recommendations, such as decapitation, cervical dislocation, or chemical injection.

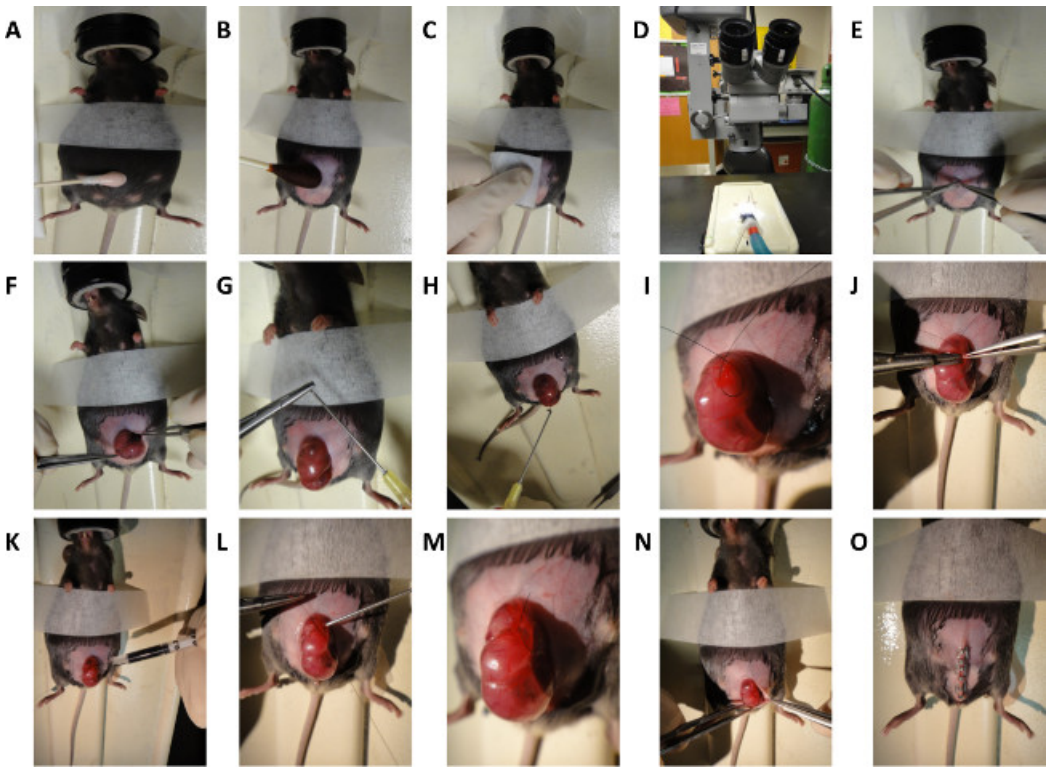

Figure 2. Schematic for Murine Fetal Surgery. General steps for dorsal wounding in E16.5 and E18.5 mouse embryos. **(A)** Depilation of mouse abdomen. **(B and C)** Preparation of mouse abdomen. **(D)** Microscope used for surgical procedure. **(E)** Midline laparotomy. **(F)** Exposure of uterus. **(G)** Creation of blunt-tip needle. **(H)** Irrigation of uterus with warm saline. **(I)** Creation of purse string suture. **(J)** Incision through uterine wall and 1 mm full thickness excisional wound generation. **(K)** Subcutaneous injection of India ink. **(L and M)** Closure of purse string suture. **(N and O)** Closure of abdomen. Please click here to view a larger version of this figure.

Representative Results

For histologic analysis, cutaneous wounds in the dorsal skin of E16.5 and E18.5 mouse embryos should be harvested 48 hr post-wounding, fixed in 4% PFA, and paraffin-embedded. In fluorescent transgenic models, cryopreservation with OCT may be appropriate. There are several stains that may be used to visualize cellular and connective tissue architecture. Hematoxylin and eosin is a two-color stain that stains nuclei blue and eosinophilic structures (*i.e.*, cytoplasm and extracellular collagen) various shades of red, pink, and orange. Mallory's trichrome is a three-color stain consisting of aniline blue, acid fuschin and orange G, best suited for distinguishing cells from surrounding connective tissue.

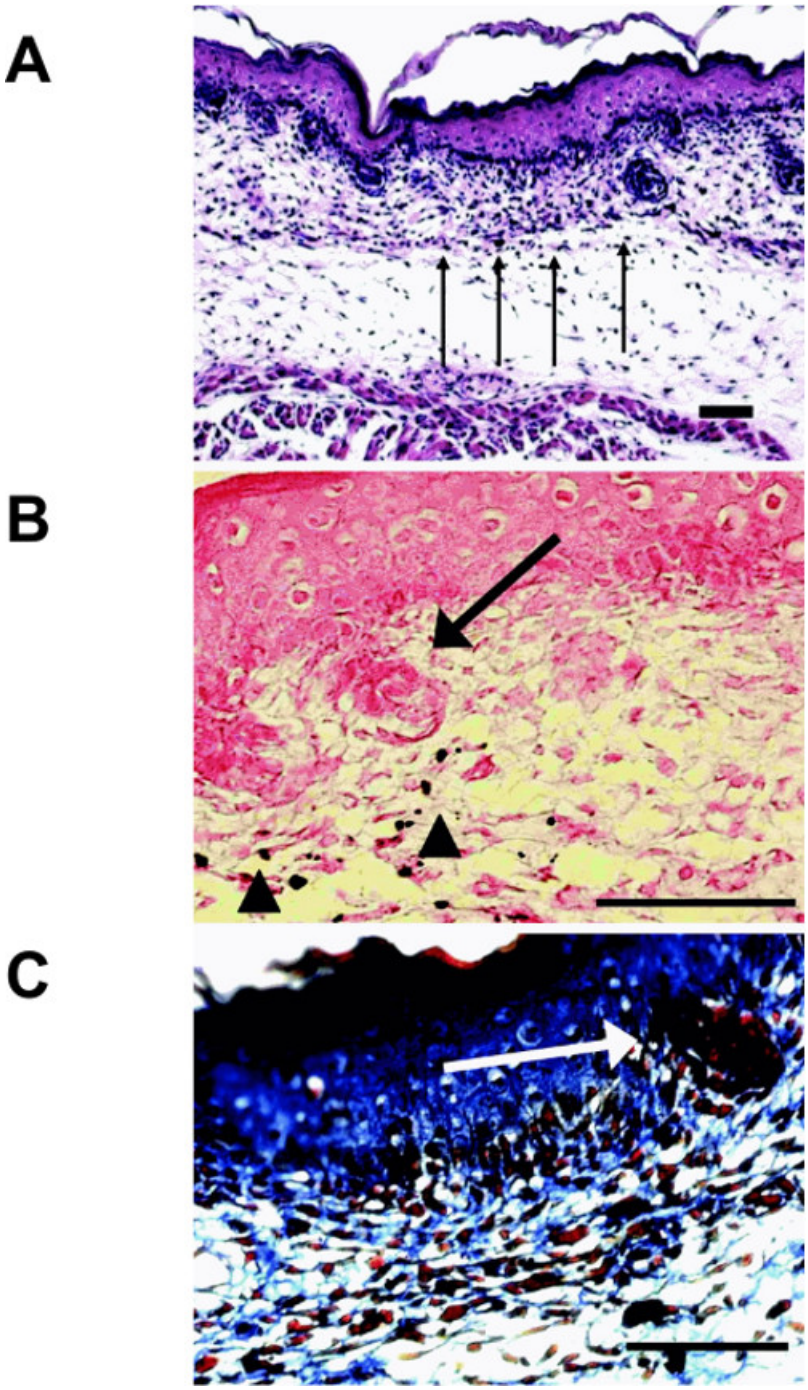

Figure 3. Histology of Scarless E16.5 Fetal Wounds. (A) Hematoxylin and eosin stain reveals complete reepithelialization and a mild increase in the number of inflammatory cells present (arrows) (100x; bar = 100 µm). **(B)** Eosin stain shows India ink (arrowheads) around regenerating hair follicles (arrow) (400x; bar = 25 µm). **(C)** Mallory's trichrome stain reveals a fine reticular dermal collagen pattern with the presence of a hair follicle (400x; bar = 25 µm). Reprinted with permission from Colwell *et al.*[10] Please click here to view a larger version of this figure.

If dorsal excisional wounds are of the appropriate size (1 mm) and depth (full-thickness), hematoxylin and eosin staining will reveal that E16.5 skin heals with minimal scarring, complete reepithelialization, and only a small increase in the number of inflammatory cells (**Figure 3A**). Moreover, these wounds should heal with approximately normal skin architecture and contain regenerating hair follicles within the site of injury (arrows; **Figure 3B**). Proper application of india ink to the freshly created wound should result in ink deposition at the site of injury (arrow heads; **Figure 3B**). Finally, trichrome staining should reveal a fine reticular dermal collagen pattern characteristic of unscarred dermis (**Figure 3C**).

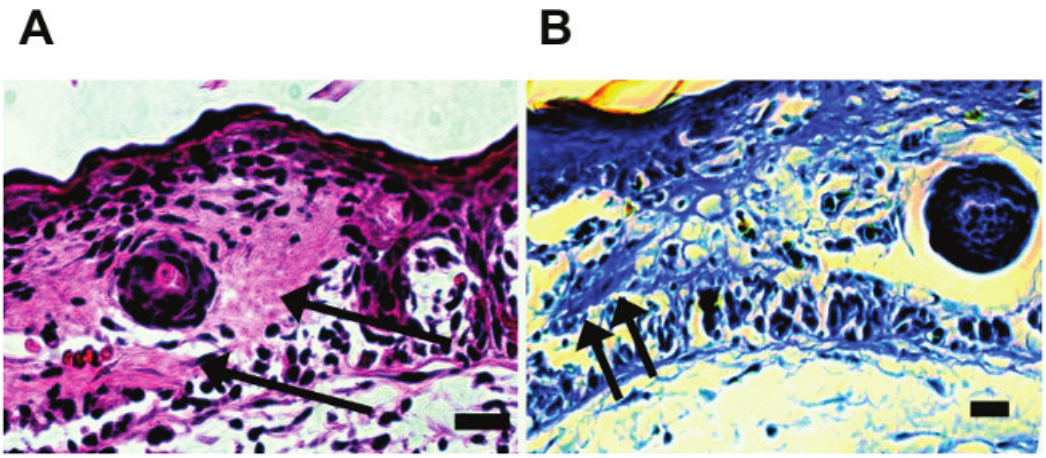

Figure 4. Histology of Scarring E18.5 Fetal Wounds. (A) Hematoxylin and eosin stain reveals an increase in eosin staining in the dermis at the site of injury (arrows) (200x; bar = 50 µm). **(B)** Mallory's trichrome stain shows dense dermal collagen (arrows) (400x; bar = 25 µm). Reprinted with permission from Colwell *et al.*[10]

In comparison to wounds made at E16.5, hematoxylin and eosin staining of dorsal wounds made at E18.5 and harvested 48 hr post-wounding should reveal a dense scar with loss of normal skin architecture at the site of injury (**Figure 4A**). Similarly, trichrome staining reveals a dense pattern of disorganized collagen deposition (arrows; **Figure 4B**). Please click here to view a larger version of this figure.

Discussion

The surgical protocol presented here describes an excisional model of fetal murine scarless healing first published in 2006 by our laboratory[10]. In addition to other established models of excisional wounding[11], incisional models of fetal murine scarless healing exist as well[12,13]. Investigations of fetal scarless wound healing in the monkey, lamb, rabbit, opossum, and rat have been reported[14-17]. However, mice represent an ideal model for exploring fetal scarless wound healing due to their comparatively low per-diem cage cost and well-characterized genome. Moreover, temporal and spatial genetic loss/gain of function can be achieved during embryonic development using murine transgenic systems offering opportunities to precisely decipher the mechanisms of scarless repair.

Despite these advantages, mice present certain technical challenges during fetal surgery due to their small size. Given the stress of anesthesia on a pregnant mother, great care should be taken to monitor the level of isoflurane/oxygen being administered. A mixture of 2.5% isoflurane/oxygen at 2 L per min followed by maintenance anesthesia at 1 L per min should be carefully adhered to. Deviations or fluctuations in this critical factor can significantly impact morbidity. Proper placement of the purse string suture represents the most technically challenging aspect of the surgery. Failure to place this stitch correctly will result in leaking of amniotic fluid and PBS post-closing. An inadequate volume of fluid in the uterus will result in trauma to the embryos and may induce premature uterine contraction. For this reason, replacement of amniotic fluid lost upon opening of the uterus is also a critical step in this surgical model. Care must be taken to continually eject warm PBS as the purse string is closed. These factors required significant troubleshooting and we emphasize that attention to these details will increase the likelihood of a successful surgery. However, even those with experienced surgical hands should plan for a morbidity rate of approximately 40% in E16.5 fetuses.

Understanding fetal scarless wound healing holds value for translational medicine aimed at *in vivo* modulation of fibrogenic behavior during adult stages of development. In comparison to adult skin, fetal skin has a developing dermis, reduced tensile strength, nascent hair follicles, and different ECM components[2,4]. Fetal skin has an elevated ratio of collagen type III to type I in comparison to adult skin, fewer and less mature mast cells, expression of Keratins 8 and 19, and higher levels of hyaluronic acid in comparison to adult skin[4,9]. By deciphering the mechanisms underlying scarless healing in the fetus, we can begin to steer the molecular and cellular pathways responsible for fibrosis in the adult towards a regenerative phenotype. The emergence of lineage tracing and other genetic tools in the mouse have opened promising new avenues for investigation of fetal scarless wound healing. Given the inherently high rates of morbidity and premature uterine contraction associated with fetal surgery, investigations of fetal scarless skin wound healing *in vivo* require a precise and repeatable surgical model. Here we detail a reproducible model of fetal scarless wound healing in the dorsum of E16.5 (scarless) and E18.5 (scarring) mouse embryos.

Disclosures

The authors have nothing to disclose.

Acknowledgements

This work was supported in part by a grant from NIH grant R01 GM087609 (to H.P.L.), a Gift from Ingrid Lai and Bill Shu in honor of Anthony Shu (to H.P.L.), NIH grant U01 HL099776 (to M.T.L.), the Hagey Laboratory for Pediatric Regenerative Medicine and The Oak Foundation (to M.T.L. and H.P.L.). G.G.W. was supported by the Stanford School of Medicine, the Stanford Medical Scientist Training Program, and NIGMS training grant GM07365. M.S.H. was supported by CIRM Clinical Fellow Training Grant TG2-01159. W.X.H. was supported by funding from the Sarnoff Cardiovascular Foundation.

References

1. Larson, B. J., Longaker, M. T., & Lorenz, H. P. Scarless fetal wound healing: a basic science review. *Plastic and reconstructive surgery.* **126**, 1172-1180, doi:10.1097/PRS.0b013e3181eae781 (2010).
2. Wilgus, T. A. Regenerative healing in fetal skin: a review of the literature. *Ostomy/wound management.* **53**, 16-31; quiz 32-13 (2007).
3. Wulff, B. C. *et al.* Mast cells contribute to scar formation during fetal wound healing. *The Journal of investigative dermatology.* **132**, 458-465, doi:10.1038/jid.2011.324 (2012).
4. Lorenz, H. P., & Adzick, N. S. Scarless skin wound repair in the fetus. *The Western journal of medicine.* **159**, 350-355 (1993).
5. Longaker, M. T. *et al.* Wound healing in the fetus. Possible role for inflammatory macrophages and transforming growth factor-beta isoforms. *Wound repair and regeneration : official publication of the Wound Healing Society [and] the European Tissue Repair Society.* **2**, 104-112, doi:10.1046/j.1524-475X.1994.20204.x (1994).
6. Longaker, M. T. *et al.* Studies in fetal wound healing. IV. Hyaluronic acid-stimulating activity distinguishes fetal wound fluid from adult wound fluid. *Annals of surgery.* **210**, 667-672 (1989).
7. Colombo, J. A., Napp, M., Depaoli, J. R., & Puissant, V. Trophic influences of human and rat amniotic fluid on neural tube-derived rat fetal cells. *International journal of developmental neuroscience : the official journal of the International Society for Developmental Neuroscience.* **11**, 347-355 (1993).
8. Colwell, A. S., Longaker, M. T., & Peter Lorenz, H. Identification of differentially regulated genes in fetal wounds during regenerative repair. *Wound repair and regeneration : official publication of the Wound Healing Society [and] the European Tissue Repair Society.* **16**, 450-459, doi:10.1111/j.1524-475X.2008.00383.x (2008).
9. Hu, M. S. *et al.* Gene expression in fetal murine keratinocytes and fibroblasts. *The Journal of surgical research*, doi:10.1016/j.jss.2014.02.030 (2014).
10. Colwell, A. S., Krummel, T. M., Longaker, M. T., & Lorenz, H. P. An *in vivo* mouse excisional wound model of scarless healing. *Plastic and reconstructive surgery.* **117**, 2292-2296, doi:10.1097/01.prs.0000219340.47232.eb (2006).
11. Wilgus, T. A. *et al.* The impact of cyclooxygenase-2 mediated inflammation on scarless fetal wound healing. *The American journal of pathology.* **165**, 753-761, doi:10.1016/S0002-9440(10)63338-X (2004).
12. Iocono, J. A., Ehrlich, H. P., Keefer, K. A., & Krummel, T. M. Hyaluronan induces scarless repair in mouse limb organ culture. *Journal of pediatric surgery.* **33**, 564-567 (1998).
13. Chopra, V., Blewett, C. J., & Krummel, T. M. Transition from fetal to adult repair occurring in mouse forelimbs maintained in organ culture. *Wound repair and regeneration : official publication of the Wound Healing Society [and] the European Tissue Repair Society.* **5**, 47-51, doi:10.1046/j.1524-475X.1997.50111.x (1997).
14. Adzick, N. S., & Longaker, M. T. Animal models for the study of fetal tissue repair. *The Journal of surgical research.* **51**, 216-222 (1991).
15. Block, M. Wound healing in the new-born opossum (Didelphis virginianam). *Nature.* **187**, 340-341 (1960).
16. Longaker, M. T., Dodson, T. B., & Kaban, L. B. A rabbit model for fetal cleft lip repair. *Journal of oral and maxillofacial surgery : official journal of the American Association of Oral and Maxillofacial Surgeons.* **48**, 714-719 (1990).
17. Longaker, M. T. *et al.* A model for fetal cleft lip repair in lambs. *Plastic and reconstructive surgery.* **90**, 750-756 (1992).

